Gross morphology of the African lion (*Panthera leo*) heart

Carmen Alicia Marais | Martina Rachel Crole

Department of Anatomy and Physiology, Faculty of Veterinary Science, University of Pretoria, Onderstepoort 0110, South Africa.

Carmen A. Marais. Department of Anatomy and Physiology, Faculty of Veterinary Science, University of Pretoria, Onderstepoort 0110, South Africa. E-mail: maraiscarmen15@gmail.com

The anatomy of the African lion heart is not well documented, and assumptions are made that the anatomy is comparable to that of the domestic cat. The increasing demand for veterinary intervention in the African lion warrants sound anatomical knowledge of the heart. The heart is situated caudal to the thoracic limbs between ribs 4-6. It is covered by the left cranial lung lobe, and cranial and middle lobe of the right lung, respectively, with a prominent cardiac incisure present on the right. Two pericardial ligaments are present, the *A. coronaria dextra* is dominant, and the *Atrium dextrum* and *Auricula dextra* possess a vast network of *Mm. pectinati*. The massive thoracic limbs, adapted to bring down prey, appear to restrict the cranial thoracic cavity, and as a trade-off, the thoracic viscera are situated more caudally. During intense activity, the heart and lungs compete against each other for space, thus limiting physical activity to short, intense periods. Capacity for sudden increase of cardiac output is facilitated by the extensive *Mm. pectinati* of the *Atrium dextrum*. Intracardiac injection is recommended on the right, ventrally in intercostal space 5. The two pericardial ligaments may help to stabilise the heart during intense activity.

Keywords
Anatomy; African lion; Heart; Thorax; Topography

1 | INTRODUCTION

Most felid species are listed by the Convention of International Trade of Endangered Species of Wild Fauna and Flora (CITES) as threatened or endangered (Davis et al., 2010). The African lion is grouped by CITES with other big cats including the tiger (*Panthera tigris*), leopard (*P. pardus*), snow leopard (*P. uncia*), jaguar (*P. onca*) and closely related clouded leopard (*Neofelis nebulosa*) (Davis et al., 2010). The International Union for Conservation of Nature (IUCN) has classified the African lion as vulnerable on their Red list (Bauer & Van Der Merwe, 2004). The population of this species is decreasing rapidly (Barnett et al., 2006) with estimates from the IUCN that mature individuals number between 23000 and 39000 (Bauer et al., 2016). Despite their dwindling numbers, trophy hunting of lions remains a major source of income for southern African countries (Lindsey et al., 2006). The hunting of larger-sized animals in the past few years has led to population dynamic changes indicated by a decrease in male numbers and a resulting male to female sex-ratio shift of 1:3 to 1:6 (Loveridge et al., 2007). Trophy hunting is described by some as key to conservation efforts by providing the financial support for conservation strategies (Lindsey et al., 2007b). Ecotourism forms an important enterprise in South Africa and tourists from around the world are attracted by the prospect of seeing the “big five” (Lindsey et al., 2007a), which includes the African lion.

The domestic cat (*Felis silvestris catus*) is an important species in the companion animal veterinary industry, has subsequently been extensively researched (Crouch, 1969; Hudson & Hamilton, 1993) and is often compared with the canine (Boyd et al., 1991; Thrall & Robertson, 2011). The anatomy of the domestic cat is most commonly used as a reference point in studies involving lions and other big cat species (Hartman et al., 2013). However, the problem with this assumption is the marked difference in size between these animals, which could lead to structural differences from a disruption of volume to surface area ratio (a small domestic cat has a larger surface area to volume ratio than that of a big cat species). It is thus important to identify the anatomical differences and similarities between the lion and domestic cat, with existing evidence suggesting that some anatomical differences are apparent (Luckhaus, 1969; Peters & Hast, 1994; Weissengruber et al., 2002; Kirberger et al., 2005a, b; Hartstone-Rose et al., 2012; Novales et al., 2015), and that the anatomy of the lion does not merely reflect an enlarged version of the domestic cat.

The veterinary treatment of lions is expanding (AZA Lion Species Survival Plan, 2012; Steeil et al., 2013; Chaos the lion, 2019) and it is important to know the topography of the African lion heart to ensure adequate veterinary intervention and humane hunting. For trophy hunting of lions, the preferred shot would be one directed at the vital organs such as the heart and or lungs to ensure that a single shot would humanely

kill the animal. It is noted in hunting guides that the position of the heart in the lion is more caudal than that of antelope (Heath, 2019). There are limited studies based on the normal cardiac anatomy of the lion with the focus on neonates (Macdonald & Johnstone, 1995) or anomalies in lion hearts and other large feline species (Franklin, 1946; Goldin & Lambrechts, 1999).

This study enhances the limited literature on the thoracic organs of the lion by providing a description of the heart of the African lion to support the increasing demand for veterinary treatment and surgery in this important zoo and wildlife species.

2 | MATERIALS AND METHODS

Three female and two male, captive bred lions of approximately 3 years of age, were culled on a private game farm in South Africa. The lions were enticed by bait and darted with a mixture of zolazepam and tiletamine by a registered veterinarian (Hartman et al., 2013). The lions were exsanguinated via the common carotid artery until cardiac arrest was achieved (Hartman et al., 2013). They were embalmed on-site with a 4% formaldehyde solution, then transported, to the Faculty of Veterinary Science, University of Pretoria where they were stored in 10% formalin baths.

The cadavers were rinsed in running tap water for 5-7 days prior to dissection. The three female lions that were used in a previous study (Hartman et al., 2013) had the abdomen opened and the hindlimbs removed. The two male specimens were intact. For dissection of the thorax, each cadaver was skinned, and the cutaneous muscles removed, from the neck region towards the 13th rib. To remove the thoracic limb the extrinsic muscles were each transected and reflected and the connective tissue, blood vessels and nerves of the brachial plexus also transected. The muscles of the thorax were sequentially removed, including the *M. iliocostalis*. The *M. rectus abdominis* and *M. obliquus abdominis externus* were reflected caudally. The extent of the pleural cavity was determined and the level of pleural reflection visualised by sequentially removing the intercostal muscles and costal pleura. The basal edge of the lungs, dome of the diaphragm and diaphragmatic line of pleural reflection were determined with the ribs *in situ* and each individually drawn on the ribs with different coloured chalk. After these landmarks were determined, the ribs were individually cut with gardening shears except for ribs 3, 7 and 11, which were only removed when the lungs were removed. Before removal of the lung, the lobes were reflected to dissect the structures within the mediastinum. Each lung was removed by transecting the *Lig. pulmonale sinister/dexter* and the *Hilus pulmonis*. This procedure was used for both the left and right side of the 2 male lion cadavers. The larger deposits of fat surrounding the pericardium were removed. After the topographical location of the heart and other cardiovascular structures were determined, the heart was removed from the pericardial sac by making two incisions in a cross-shape pattern over the middle of the fibrous pericardium to reflect the four quarters, and transecting the *Aorta, V. cava cranialis* and *V. cava caudalis*.

One female cadaver was opened from both the left and the right sides to note the topography before the entire content of the thoracic cavity was removed intact. The remaining two female cadavers were opened from the right side and the individual organs (heart and lungs) removed intact. The following structures were transected to facilitate removal of the thoracic viscera: *V. cava caudalis*, pulmonary ligaments, pericardial ligaments, trachea, esophagus, all the blood vessels and nerves cranial to the heart and connective tissue / mediastinum. In the two male cadavers, the lungs were first separated from the heart, and the heart dissected individually, whereas the hearts from the three female cadavers were dissected while remaining connected to the lungs.

The fat filling the coronary and interventricular grooves and *Basis cordis* was removed to expose significant structures. The heart was opened on the left by incising immediately caudal to the *Auricula sinistra* from the *Basis cordis* to the *Apex cordis* so as to expose the *Atrium sinistrum* and *Ventriculus sinister*. On the right side, two incisions were made to expose the internal structures. A more cranially situated diagonal incision was made throughout the *Conus arteriosus* from the point of the *Valva trunci pulmonalis* to the region of the *Apex cordis*. The second incision was made more caudally. This longitudinal incision ran from the *Basis cordis* to the *Apex cordis* through the middle of the *Atrium dextrum* and *Ventriculus dexter* from the level of the *V. cava cranialis*. In some specimens, the entire left and right atria were removed to expose the heart valves and demonstrate the blood supply to the chambers. This was performed by making a horizontal incision through the atria and auricles. The atrium of each side was then removed by cutting along the heart wall at the level of the *Sulcus coronarius* just dorsal to the vessels. The remaining connections were transected at the level of the *Bulbus aortae*. The *Tr. pulmonalis* and *Aorta* were trimmed up to the level of the semilunar valves.

Structures were described, digital macrographs were captured with a Canon IXUS 115 HS Full HD, 12.1 megapixel camera (Canon, Japan) and Samsung Galaxy S9+ and Samsung Galaxy S6 smartphones (Samsung Electronics, Vietnam) and annotated with CorelDRAW X5.

The terminology used for this study is based on that of Illustrated Veterinary Anatomical Nomenclature (Schaller, 1991) and Nomina Anatomica Veterinaria 5th Edition (Revised) (ICVGAN, 2012).

3 | RESULTS

3.1 | Topography

The cranial portion of the thoracic cavity is narrowed dorso-ventrally and medio-laterally, reflected in the shape of the cranial lung lobes. Viewed dorsally there is a marked increase in diameter from cranial to caudal

and the thoracic cavity is shaped like an isosceles triangle with the apex facing cranially. The tricipital line extends over rib 4 with little lung tissue present between ribs 1-4. The heart is situated between ribs 4 and 6 and the 6th intercostal space and lies entirely caudal to the tricipital line. The longitudinal axis is tilted 60° from the vertical axis. This causes the *Basis cordis* to be situated dorso-cranially with the *Apex cordis* lying more caudo-ventrally. The *Apex cordis* is positioned medial to the angle of the 6th rib and extends slightly into the 6th intercostal space. The left surface of the heart (*Facies auricularis*) is in contact with the medial surface of the cranial and caudal parts of the cranial lobe of the left lung. The right surface of the heart (*Facies atrialis*) is partly covered by the caudal part of the medial surface of the right cranial and middle lung lobes. The larger right *Incisura cardiaca* in the ventral margin of the right lung, allows greater contact of the *Ventriculus dexter* with the *Pleura costalis* than the comparable structures on the left.

The heart is suspended in the middle mediastinum by the major blood vessels and bronchi. The first few *Aa. intercostales dorsales* originating from the thoracic aorta are directed cranially, creating the impression that the heart and proximal arteries are retracted caudally. The lions used for this study were juvenile animals when culled, thus the thymus is visible on the cranial border of the heart.

The *Valva trunci pulmonalis*, on the left, is positioned caudal to the tricipital line at the fourth intercostal space, midway between the angle and the genu of the rib. The *Valva aortae* is slightly more dorsal in the 5th intercostal space. The *Valva atrioventricularis sinistra* (mitral valve) is in the 6th intercostal space approximately 2 cm dorsal to the costochondral junction of rib 6. The *Valva atrioventricularis dextra* (tricuspid valve), on the right, is similar in location to that of the mitral valve and is present in the 6th intercostal space approximately 2 cm dorsal to the costochondral junction of rib 6.

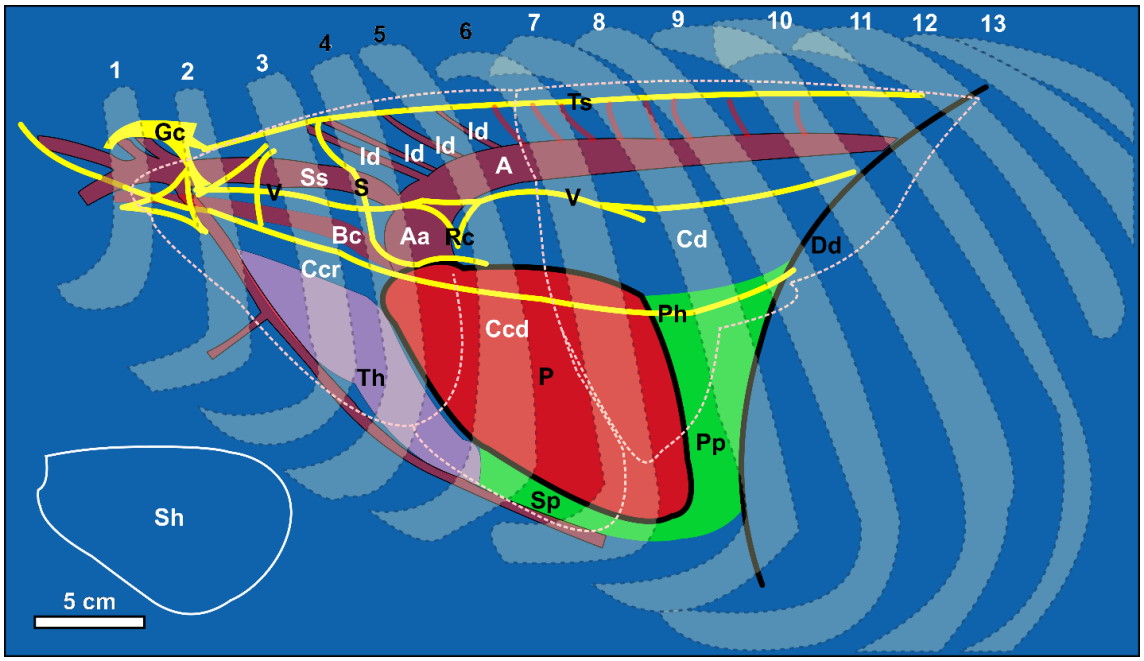

FIGURE 1 Schematic representation of the topography of the thoracic organs and structures, left lateral, with a slight cranial-oblique view. The ribs (dotted outline and pale white shading) are depicted from the genu to the joint with the sternum and numbered from 1-13. The inserted white outline (Sh) demonstrates the angular and irregular shape of the rib cage and is not to scale. Organs and structures: Thymus (Th, pink), pericardium (P, red), *Lig. sternopericardiacum* (Sp, green), *Lig. phrenicopericardiacum* (Pp, green), left lung (white dotted outline): cranial part of the cranial lobe (Ccr), caudal part of the cranial lobe (Ccd) and caudal lobe (Cd), dome of the diaphragm (Dd). Arteries: *Arcus aortae* (Aa), *Aorta ascendens* (A), *Tr. brachiocephalicus* (Bc), *A. subclavia sinistra* (Ss), *Aa. intercostales dorsales* (Id). Nerves (yellow lines): *Ggl. cervicothoracicum* (Gc), *N. vagus* (V), *Rr. cardiaci* (Rc), sympathetic nerves (S), *Tr. sympathicus* (Ts), *N. phrenicus* (Ph).

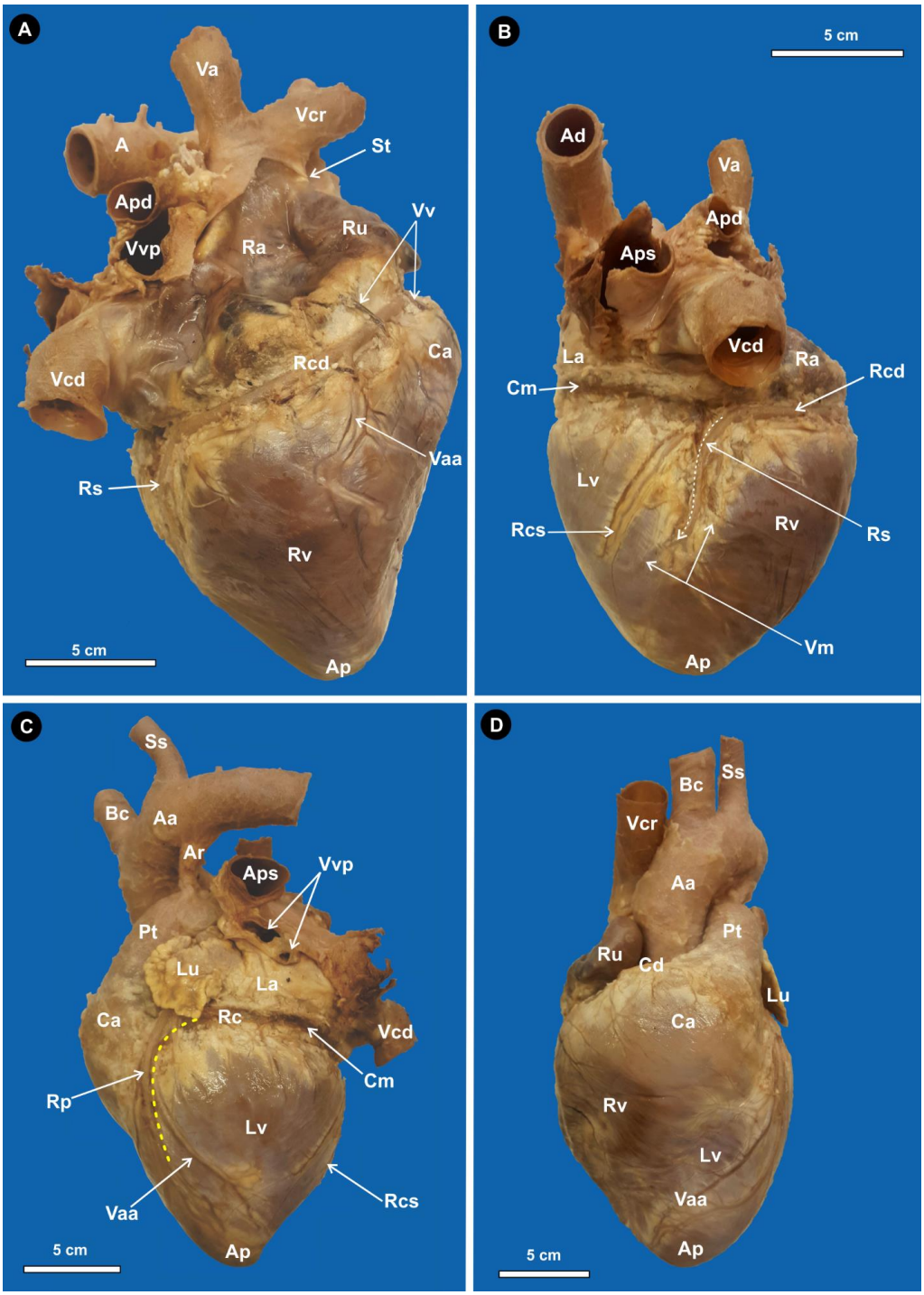

FIGURE 2 External features of the heart. **(A):** Right lateral view, *Facies atrialis*. The *A. coronaria dextra* is visible in the *Sulcus coronarius* with small ventricular arteries on the *Ventriculus dextra* running ventrally toward the *Apex cordis*. The *Venae cordis dextrae* run over the *R. circumflexus* of the *A. coronaria dextra*. **(B):** Caudal view. The left and right ventricles are separated by the *Sulcus interventricularis subsinuosus*. The *V. cordis magna* and the *A. coronaria dextra* are visible in the coronary groove dorsal to the left ventricle and right ventricle, respectively. The *Ramus intermedius* of the *V. cordis magna* and the *Ramus intermedius* of the *A. coronaria dextra* run together on the *Ventriculus sinister* and do not reach the *Apex cordis*. **(C):** Left lateral view, *Facies auricularis*. Note the *Tr. pulmonalis* with the *Lig. arteriosum* connected to the *Arcus aortae*. **(D):** Cranial view. This figure shows that the *Apex cordis* is part of the *Ventriculus sinister*. **Glossary:** *A. coronaria dextra* (Cd): *R. circumflexus* (Rcd), *R. interventricularis subsinuosus* (Rs), *R. coronaria sinistra* (Rcs); *A. coronaria sinistra*: *R. interventricularis paraconalis* (Rp), *R. circumflexus* (Rc); *Aorta* (A), *Aortae descendens* (Ad), *Apex cordis* (Ap), *A. pulmonis sinistra* (Aps), *A. pulmonis dextra* (Apd), *Arcus aortae* (Aa), *A. subclavia sinistra* (Ss), *Atrium dextrum* (Ra), *Atrium sinistrum* (La), *Auricula dextra* (Ru), *Auricula sinistra* (Lu), *Conus arteriosus* (Ca), *Lig. arteriosum* (Ar), *Sulcus terminalis* (St), *Sulcus interventricularis paraconalis* (yellow dashed line), *Sulcus interventricularis subsinuosus* (white dashed line), *Tr. brachiocephalicus* (Bc), *Tr. pulmonalis* (Pt), *V. azygos dextra* (Va), *V. cava caudalis* (Vcd), *V. cava cranialis* (Vcr), *V. cordis magna* (Cm), *V. cordis media* (Vm), Ventricular arteries (Vaa), *Ventriculus dexter* (Rv), *Ventriculus sinister* (Lv), *Vv. cordis dextrae* (Vv) and *Vv. pulmonis* (Vvp).

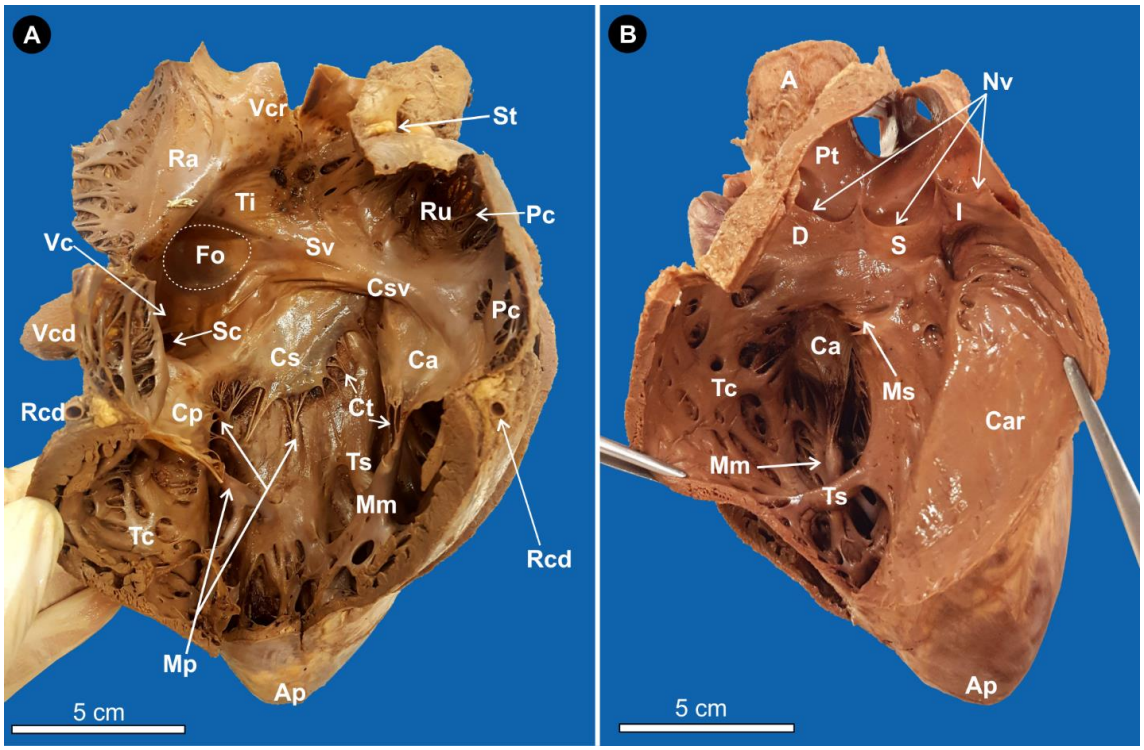

FIGURE 3 The right side of the heart opened and reflected to demonstrate the internal features of the *Atrium dextrum* and *Ventriculus dextra*. **(A):** Right lateral view. Note how the prominent *Mm. pectinati* are not limited to the region of the *Auricula dextra*. Ventral to the *Fossa ovalis*, the *Sinus coronarius* is visible with its distinct *Valvula sinus coronarii*. The *M. papillaris magnus* is connected to the *Cuspis angularis* via the *Chordae tendineae*. **(B):** Cranial view. The *Conus arteriosus* is reflected to demonstrate *Valva trunci pulmonalis* / *Lunulae valvularum semilunarium*, namely the *Valvula semilunaris intermedia, dextra* and *sinistra*. **Glossary**: *A. coronaria dextra*: *R. circumflexus* (Rcd), *Aorta* (A), *Apex cordis* (Ap), *Atrium dextrum* (Ra), *Auricula dextra* (Ru), *Chordae tendineae* (Ct), *Conus arteriosus* (Car), *Crista supraventricularis* (Csv), *Cuspis angularis* (Ca), *Cuspis parietalis* (Cp), *Cuspis septalis* (Cs), *Fossa ovalis* (Fo) (encircled in white dashes), *M. papillaris magnus* (Mm), *Mm. papillares parvi* (Mp), *M. papillaris subarteriosus* (Ms), *Mm. pectinati* (Pc), *Noduli valvularum semilunarium* (Nv), *Sinus coronarius* (Sc), *Sinus venarum cavarum* (Sv), *Sulcus terminalis* (St), *Trabeculae carnea* (Tc), *Trabecula septomarginalis dextra* (Ts), *Tr. pulmonalis* (Pt), *Tuberculum intervenosum* (Ti), *V. cava cranialis* (Vcr), *V. cava caudalis* (Vcd), *Valva trunci pulmonalis* / *Lunulae valvularum semilunarium* (Ls)*: Valvula semilunaris intermedia* (I)*, dextra* (D) and *sinistra* (S) and *Valvula sinus coronarii* (Vc).

3.2 | Pericardium

The pericardium is thick, fibrous and contains a large quantity of yellow fat at the region of the *Apex cordis*. The result is that the *Apex cordis* appears to extend much further caudally than it does. Ventrally and caudally, the *Pericardium fibrosum* forms broad attachments to the sternum (*Lig. sternopericardiacum*) and diaphragm (*Lig. phrenicopericardiacum*) (Figure 1), respectively. The *Lig. sternopericardiacum* is more delicate than the *Lig. phrenicopericardiacum*. At the *Basis cordis*, the *Pericardium fibrosum* continues onto the large blood vessels, forming the *Sinus transversus*. This is an extension of the *Cavum pericardii* between the major blood vessels and the atria and is mostly fat-filled. The *Lamina visceralis* of the *Pericardium serosum* forms the epicardium and with the *Lamina parietalis*, the *Cavum pericardii*.

3.3 | External features

The *Basis cordis* faces dorso-cranially and accommodates all the major arteries and veins (Figures 2-4). The *Apex cordis* is blunt and directed caudo-ventrally towards the sternum and diaphragm and forms the distal extremity of the *Ventriculus sinister* (Figures 2-4). The atria (*Atrium cordis*) are situated dorsal to the ventricles (*Ventriculus cordis*) and are located opposite each other on either side of the median plane (Figures 2A and 2C). The ventricles are similarly arranged with the result that the *Facies auricularis*, or left surface of the heart, displays the small, rounded *Auricula sinistra*, small *Atrium sinistrum*, *Ventriculus sinister* and the *Conus arteriosus* (Figure 2C). The *Facies atrialis*, or right surface of the heart, displays the *Atrium dextrum*, *Auricula dextra* and *Ventriculus dexter* (Figure 2A). The *Auricula sinistra* is located in the left 5th intercostal space just caudal to the *Tr. pulmonalis* and is covered laterally by the *Lobus cranialis* of the left lung (Figure 1). It is bordered cranially by the *Tr. pulmonalis* and ventrally by the *R. circumflexus* of the *A. coronaria sinistra* and *V. cordis magna* (Figure 2C). The larger, triangular-shaped *Auricula dextra* (Figure 2A), is located in the right 4th intercostal space and is covered laterally by the *Lobus cranialis* of the right lung. The dorsal border is marked by the *Sulcus terminalis* and the ventral border by the *Sulcus coronarius* (Figure 2A). The apex of the triangle is visible on the *Margo cranialis*, lateral to the *Arcus*

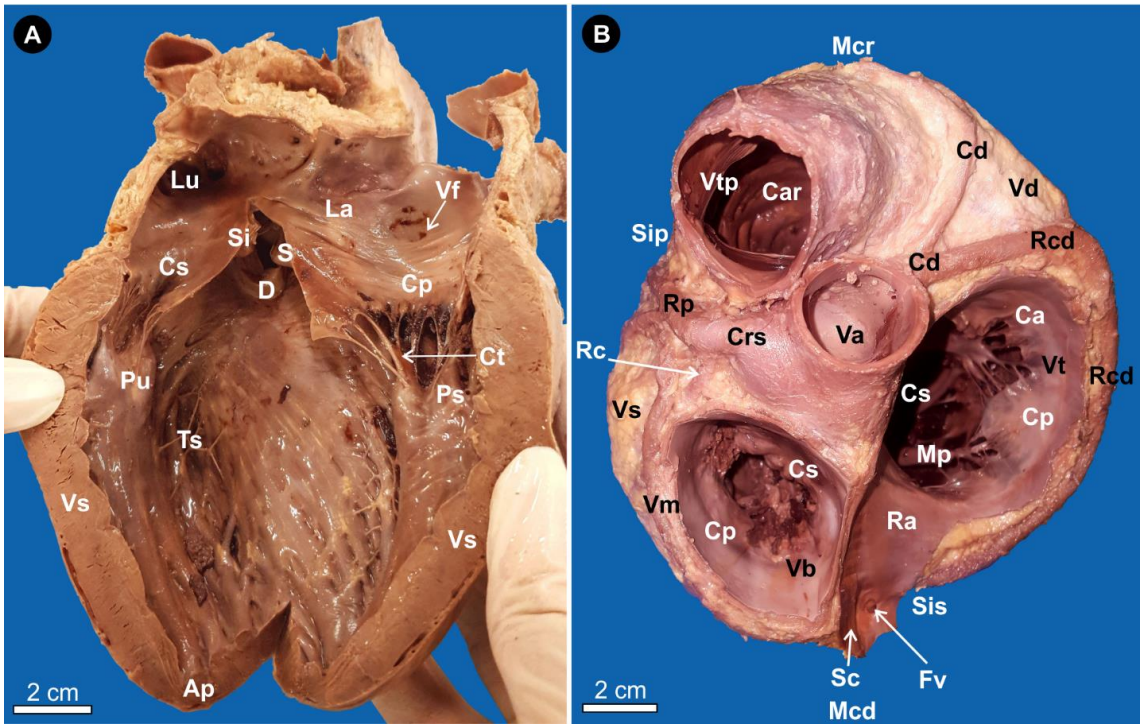

FIGURE 4 (A): The left side of the heart opened and reflected to demonstrate the internal features of the *Atrium sinistrum* and *Ventriculus sinister*. The *Ostium atrioventriculare sinistrum* is closed by the *Cuspis septalis* and *Cuspis parietalis*. The *Valvae aortae* is composed of the *Valvula semilunaris septalis / dextra / sinistra*. **(B):** Dorsal view of the heart. Atria removed. Note the larger *A. coronaria dextra* and the smaller *A. coronaria sinistra*. **Glossary:** *A. coronaria dextra* (Cd): *R. circumflexus* (Rcd); *A. coronaria sinistra* (Crs): *R. interventricularis paraconalis* (Rp), *R. circumflexa* (Rc); *Apex cordis* (Ap), *Atrium dextrum* (Ra), *Atrium sinistrum* (La): *Ostium atrioventriculare sinistrum* with the *Cuspis septalis* (Cs) (cut) and *Cuspis parietalis* (Cp); *Auricula sinistra* (Lu), *Chordae tendineae* (Ct), *Conus arteriosus* (Car), *Forr. venarum minimarum* (Fv), *Mm. papillares parvi* (Mp), *M. papillaris subatrialis* (Ps), *M. papillaris subauricularis* (Pu), *Margo cranialis* (Mcr), *Margo caudalis* (Mcd), *Sinus coronarius* (Sc), *Sulcus interventricularis paraconalis* (Sip), *Sulcus interventricularis subsinuosus* (Sis), *Trabecula septomarginalis* (Ts), *V. cordis magna* (Vm), *Valva aortae* (Va), *Valva bicuspidalis* (Vb) with the *Cuspis septalis* (Cs) and *Cuspis parietalis* (Cp); *Valva tricuspidalis* (Vt) with the *Cuspis septalis* (Cs) (not visible), *Cuspis parietalis* (Cp) and *Cuspis angularis* (Ca); *Valva trunci pulmonalis* (Vtp), *Valvula foraminis ovalis* (Vf), *Valvula semilunaris dextra* (D), *Valvula semilunaris septalis* (S) and *Valvula semilunaris sinistra* (Si), *Ventriculus dextra* (Vd), *Ventriculus sinister* (Vs).

aortae (Figure 2D). The *Margo ventricularis dexter* (cranial margin) is composed of the *Conus arteriosus* of the *Ventriculus dexter*, which is the main contributor to the cranial margin, and by a small part of the *Ventriculus sinister* (Figure 2D). The *Margo ventricularis sinister* (caudal margin) is composed of both the *Ventriculus sinister* and *Ventriculus dexter* separated in the middle by the *Sulcus interventricularis subsinuosus* (Figure 2B). The latter, with its accompanying blood vessels, is positioned ventral to the *V. cava caudalis* (Figure 2B).

The *Sulcus interventricularis paraconalis*, which separates the two ventricles on the left surface, originates ventral to the *Auricula sinistra,* just caudal to the *Tr. pulmonalis* (Figure 2C). The *Sulcus*B *interventricularis paraconalis* does not reach the *Apex cordis*; however, the *R. interventricularis paraconalis* ofC the *A. coronaria sinistra* terminates close to it. The *Sulcus interventricularis subsinuosus* is visible on the caudal margin of the heart (Figure 2B). It originates just ventral to, and in line with the point where the *V. cava caudalis* empties into the *Atrium dextrum* (Figure 3A) and, similar to the *Sulcus interventricularis paraconalis*, does not reach the *Apex cordis*. The caudal positioning of the *Sulcus interventricularis subsinuosus* indicates that the *Ventriculus sinister* occupies the left side of the heart only. The interventricular grooves and the *Sulcus coronarius* are filled with soft, yellow fat. The *Sulcus coronarius* is a horizontal indentation that originates just ventral to the *Auricula sinistra*, caudal to the *Conus arteriosus,* from where it continues over the entire caudal surface of the heart separating the atria from the ventricles (Figure 2). It continues on the right surface of the heart to just caudal to the *Conus arteriosus*, ventral to the *Auricula dextra*. The *V. cordis magna* and left and right *R. circumflexus* of the respective coronary arteries are present in the *Sulcus coronarius* (Figures 2A-C and 4B).

3.4 | Structure of the heart chambers

3.4.1 | *Right atrium*

The *Atrium dextrum* is comprised of the *Sinus venarum cavarum* caudally and the *Auricula dextra* cranially (Figure 3A). The *V. cava cranialis* and *caudalis* drain into the *Sinus venarum cavarum* (Figure 3A) while the *V. azygos dextra* opens into the *V. cava cranialis* before draining into the *Atrium dextrum* (Figure 3A). The *Tuberculum intervenosum* forms a ridge which leads to

the smooth surface of the *Sinus venarum cavarum*, terminating before the *Crista supraventricularis* (Figure 3A). *Valvula venae cavae caudalis* are absent. The *Sulcus terminalis* is very distinct as the *V. cava cranialis* enters the *Atrium dextrum* at an angle of almost 90° (Figures 2A and 3A). The interior ridge of the *Sulcus terminalis*, the *Crista terminalis*, is very thin and surrounded by the *Mm. pectinati* (Figure 3A). The *V. cordis magna*, which drains the myocardium, opens into the *Atrium dextrum* via the *Sinus coronarius*, which is located just ventral to the *V. cava caudalis* (Figure 3A). The *Valvula sinus coronarii* is a distinct semilunar valve-like fold located just dorsal to the sinus. Closely associated with the *Sinus coronarius* are the *Forr. venarum minimarum* through which the *Vv. cordis minimae* drain into the *Atrium dextrum*. The caudo-ventral part of the *Atrium dextrum* is smooth while the cranio-lateral part, including the *Auricula dextra*, bears the prominent *Mm. pectinati* (Figure 3A). The *Mm. pectinati* are not restricted to the region of the *Auricula dextra* but are also distributed on most of the parietal wall of the *Atrium dextrum* (Figure 3A). The *Fossa ovalis* is easily visible on the partition between the atria (Figure 3A). It is smooth, oval and measures approximately 1.5 x 3 cm.

3.4.2 | *Right ventricle*

There is a marked difference in wall thickness between the ventricles. The right ventricular wall (Figure 3) is thinner than that of the left ventricle (Figure 4A). The main structural features of the *Ventriculus dexter* ventral to the *Atrium dextrum* are the cusps forming the *Valva atrioventricularis dextra*, the *Mm. papillares* and the *Chordae tendineae*. The *Ostium atrioventriculare dextrum* is identified by the three cusps forming the *Valva atrioventricularis dextra* (Figures 3 and 4B). The most medial cusp (*Cuspis septalis*) originates on the *Septum interatriale* (Figures 3A and 4B). It shares two small *Mm. papillares* with the *Cuspis parietalis*. The *Mm. papillares parvi* are situated on the septal (two) and parietal (one) wall in one of the specimens (Figures 3A and 4B). The latter muscle is a single muscle in the other 4 specimens where some *Chordae tendineae* of the *Cuspis septalis* attach directly to the *Septum interventriculare*. The smooth septal surface of the *Sinus venarum cavarum* is situated just dorsal to the *Cuspis septalis*. The most cranial cusp (*Cuspis angularis*) is present on the heart wall and septum (Figures 3 and 4B). It attaches to the *M. papillaris subarteriosus* and the *M. papillaris magnus*. Cranially, the *M. papillaris subarteriosus* originates from the septal wall and attaches to the *Cuspis angularis* and *Cuspis septalis* via the *Chordae tendineae* (Figure 3B). The *M. papillaris magnus* is the largest muscle and is situated on the parietal heart wall (Figure 3). The third cusp (*Cuspis parietalis*) is the smallest and is situated more caudally (Figures 3A and 4B). It shares *Mm. papillares* with the *Cuspis septalis* (*Mm. papillares parvi*) and the *Cuspis angularis* (*M. papillaris magnus*). The *Chordae tendineae* are thin cord-like strands which vary in length (Figure 3A). They connect the free edges of the *Valva atrioventricularis dextra* to the *Mm. papillares* and *Septum interventriculare*. The *Chordae tendineae* are longest towards the centre of each cusp and shorter towards either side of the cusp. From the attachment to the *Mm. papillares* the *Chordae tendineae* branch out to attach to different points of the various cusps.

The funnel-like *Conus arteriosus* (Figures 2A, 2C, 2D and 3B) forms the most cranial part of the heart and directs blood into the *Tr. pulmonalis* via the *Ostium trunci pulmonalis* (Figure 3B). The *Valva trunci pulmonalis* is formed by three crescent-shaped folds (Figures 3B and 4B). The *Valvula semilunaris intermedia* (transected in the specimens to reflect the *Conus arteriosus*) is the most cranial semilunar valve. The *Valvula semilunaris dextra* lies adjacent to the *Bulbus aortae* while the *Valvula semilunaris sinistra* is associated with the *Septum interatriale*. The *Noduli valvularum semilunarium* are not equally as prominent in each of these semilunar valves. The nodule is well-defined in the *Valvula semilunaris intermedia*, represented only by a small dot-like structure in the *Valvula semilunaris dextra* and is poorly defined in the *Valvula semilunaris sinistra* (Figure 3B). There is no visible difference in the *Lunulae valvularum semilunarium* of the *Tr. pulmonalis*. The wall of the *Ventriculus dexter* has prominent *Trabeculae carneae* which are not as well-defined in the *Ventriculus sinister*. They are prominent muscular ridges on the parietal wall of the ventricle and the ventral part of the septum but do not extend to the *Conus arteriosus* which has a smooth parietal wall (Figure 3). The *Trabecula septomarginalis dextra* is a thick band that stretches from the *Septum interventriculare* to the ventricular wall, cranial to the *M. papillaris magnus* (Figure 3).

3.4.3 | *Left atrium*

The *Atrium sinistrum* is smaller than the *Atrium dextrum* and is surrounded by yellow fat on the exterior surface. It is composed of a cranial *Auricula sinistra* and a caudal part (atrium) into the roof of which the pulmonary veins drain via four variably sized *Ostia venarum pulmonalium*. The *Mm. pectinati* are not as widespread as those in the *Atrium dextrum* and are only present in the region of the *Auricula sinistra*. The *Fossa ovale* presents a slight indentation on its ventral aspect representing the *Valvula foraminis ovalis* and which effectively forms the floor of the *Fossa ovale* (Figure 4A).

3.4.4 | *Left ventricle*

The wall of the *Ventriculus sinister* (Figure 4A) is substantially thicker than that of the *Ventriculus dexter* (Figure 3A). In the *Ventriculus sinister*, the *Mm. papillares* are thick and larger than in the *Ventriculus dexter*. There are two muscle groups, namely the *M. papillaris subatrialis* and the *M. papillaris subauricularis,* which lies directly ventral to the *Auricula sinistra* (Figure 4A). The *Ostium atrioventriculare sinistrum* is marked by two cusps

forming the *Valva atrioventricularis sinistra* or *Valva bicuspidalis / mitralis* (Figure 4). The *Chordae tendineae* (Figure 4A) are similar to those of the *Ventriculus dexter;* however, they connect the free edges of the *Valva atrioventricularis sinistra* only to the *Mm. papillares*. The *Cuspis septalis* arises from the septal wall and is attached to the *M. papillaris subatrialis* and *subauricularis*. The *Cuspis parietalis*B originates from the heart wall and is attached to the prominent *M. papillaris subatrialis.* There is no *Trabecula septomarginalis* in the *Ventriculus sinister*. The *Ostium aortae* comprises the *Valvae aortae* with three crescent-shaped folds (Figure 4). The *Valvula semilunaris septalis* and *Valvula semilunaris sinistra* are associated with the *Septum interatriale* positioned cranially to the *Cuspis septalis* (Figure 4). The *Valvula semilunaris dextra* is associated with the *Septum interventriculare* (Figure 4) and is positioned medial to the *Tr. pulmonalis*. Centrally positioned on the free edge of each of the triangular-shaped *Valvae aortae* is a nodular structure, the *Noduli valvularum semilunarium*, which also appears triangular when viewed from the ventral aspect of the aorta. Flanking the nodules are the *Lunulae valvularum semilunarium* which form the sides of the cusps.

3.5 | The aorta and blood supply

At the base of the aorta, the dilated *Bulbus aortae,*B marks the origin of the *Aa. coronariae* (Figure 4B). Each coronary artery forms two major branches. The *A. coronaria sinistra* runs between the *Tr. pulmonalis* and *Auricula sinistra* towards the *Sulcus coronarius* (Figures 2C and 4B). It divides to form the ventrally directed *R. interventricularis paraconalis* which runs in the *Sulcus interventricularis paraconalis* and the caudally directed *R. circumflexus* which runs in the *Sulcus coronarius* (Figures 2C and 4B). The greater portion of the *Septum interventriculare* is supplied by the *Rr. septales* directed off the *R. circumflexus*. The *R. interventricularis paraconalis* supplies the *Conus arteriosus* and the *Ventriculus sinister* and the *R. circumflexus* supplies the wall of the *Ventriculus sinister*. The *A. coronaria dextra* passes between the *Tr. pulmonalis* and the *Auricula dextra* (Figure 4B). After giving off the small *Rr. septales* and the larger *R. circumflexus,* it continues cranially and to the left around the *Conus arteriosus* where it supplies the latter. The *R. circumflexus* runs caudally in the *Sulcus coronarius* and branches into the ventrally directed *R. interventricularis subsinuosus* running in the *Sulcus interventricularis subsinuosus* (Figures 2A and 4B), and the caudo-ventrally directed *R. coronaria sinistra* (Figure 2B). The former supplies the wall of the *Ventriculus dexter,* whereas the latter supplies part of the wall of the *Ventriculus sinister*.

The *Bulbus aortae* continues dorsally as the *Aorta ascendens* before it curves caudally as the *Arcus aortae* (Figure 2). The first branch from the *Arcus aortae* is the *Tr. brachiocephalicus* (Figures 1, 2C and 2D). Just caudal to the *Tr. brachiocephalicus* the *A. subclavia sinistra* (Figures 1, 2C and 2D) originates dorsally on the *Arcus aortae* at the level of the *Lig. arteriosum,* which is present on the ventral surface of the aorta. The prominent *Lig. arteriosum* is visible on the left surface of the heart just dorsal to the *Auricula sinistra*, runs between the *Aorta* and the *Tr. pulmonalis* (Figure 2C) and measures 15 - 20 mm in length.

3.6 | Venous drainage

The *V. cordis magna* drains the blood from the cardiac walls. From the region close to the *Apex cordis* on the *Ventriculus sinister*, the *V. cordis magna* proceeds dorsally in the *Sulcus interventricularis paraconalis* and then into the *Sulcus coronarius* to the caudal edge of the heart where it drains into the *Sinus coronarius* of the *Atrium dextrum* (Figures 2B and 2C). The *V. cordis magna* is encased in a fat layer in the *Sulcus coronarius*. A collection of smaller veins on the caudal surface of the heart are the *Vv. cordis minimae* which drain through the *Forr. venarum minimarum* into the *Atrium dextrum* (Figure 3A). The *Venae cordis dextrae* are visible on the right surface of the heart (Figure 2A). They lie superficially on the *Ventriculus dexter* and proceed dorsally to the right *R. circumflexus* before entering the *Atrium dextrum*. The *Venae cordis dextrae* are small in diameter. The *Vena cordis media* follows the course of the *R. interventricularis subsinuosus* (Figure 2B).

3.7 | Innervation

The parasympathetic nerve supply from the *N. vagus* is the *Rr. cardiaci*. On the left, the *Rr. cardiaci* enter the heart just caudal to the *Arcus aortae* in the *Atrium sinistrum*. The sympathetic nerve supply from the *Gl. cervicothoracicum* on the left enters the heart at the *Atrium sinistrum,* just cranial to where the parasympathetic nerve supply enters. On the right, the *Rr. cardiaci* branch off the *N. vagus* just caudal to the *V. azygos dextra* and enter the heart in the *Atrium dextrum* just cranial to the *Vv. pulmonalis*. The sympathetic nerve supply is similar to that on the left and originates from the *Gl. cervicothoracicum* and enters the heart just cranial to where the *Rr. cardiaci* enter the *Atrium dextrum*.

4 | DISCUSSION

The heart of the large cats (*Panthera*) is very similar to that of the small cats (*Felis*) (Rowlatt, 1990). In all mammals the heart (*Cor*) is composed of four chambers and the blood supply to, and from the heart to the rest of the body, is distributed through the same main arteries and veins in all mammalian species (Rowlatt, 1990). The heart is located in the middle mediastinum, which separates the two pleural cavities (Miller et al., 1964). There are two pumps within the heart; namely, the right, which receives venous blood from the body and pumps it into the pulmonary trunk to be oxygenated by the lungs (Dyce et al., 2010), and the left, which then receives the oxygen-rich blood from the pulmonary veins and pumps it into the aorta to be distributed to the rest of the body (Dyce et al., 2010).

These features were all typically present in the African lion.

4.1 | Topography

The location of the heart in the domestic dog (*Canis familiaris*) is between ribs 3 and 6 and in the domestic cat between ribs 4 and 7 (Habel, 1978). The cranial extent of the lion heart is similar to that of the domestic cat; however, the caudal border lies somewhere between that of the domestic dog and cat. Unlike most mammals, the lion heart lies entirely caudal to the thoracic limb. The shape of the thorax of the lion was irregular and very angular (see Figure 1). In contrast, the shape of the thoracic cavity of other domestic species, such as the dog and horse, is described as being barrel-shaped (Dyce et al., 2010) or oval-shaped (Miller et al., 1964), respectively. With its massive thoracic limbs, it would appear that the cranial thoracic cavity in the lion is narrowed to allow for an increase in size of the pectoral girdle musculature. The cranial lung lobes were medio-laterally compressed in comparison to the base of the lungs (present study) thus most respiration would occur in the caudally situated lobes. This likely also reflects the large mass of the thoracic limbs that would restrict expansion of the cranial portion of the thoracic cavity. The tricipital line extended over rib 4 and very little lung tissue was present between ribs 1-4. These features of the cranial thoracic cavity affirm the function of the thoracic limbs in the African lion for bringing down large and strong prey (Hopwood, 1947). The mass and volume of the heavily muscled thoracic limbs appears to limit expansion of the cranial thorax and may explain the caudal location of the thoracic viscera. Comparing other large domestic mammals such as the bovine and horse to the lion, it is noted that the heart of the bovine and horse is located medial to the thoracic limb (Dyce et al., 2010). This offers more protection to the heart and it appears that the lion may have traded this protective function for more powerful thoracic limbs. The stomach of the lion has the capacity to store up to 20% and more of its body weight, which ensures a reduced frequency of feeding (AZA Lion Species Survival Plan, 2012). However, the full stomach would encroach on the diaphragm and further limit the already restricted space in the caudal thoracic cavity available for the heart and lungs. This may in part explain the lethargy of recently fed lions and the behaviour of lying outstretched on their backs after eating (personal observation). Such a posture may relieve the pressure of a full stomach on the diaphragm. Based on these observations it is therefore important that the stomach is empty when tranquilising and transporting lions as respiration and cardiac output could become severely compromised.

The orientation of the lion heart is more inclined at 60° compared to the 45° of the heart of the dog (Miller et al., 1964). The difference clearly indicates that the heart of the lion is positioned more obliquely in the thoracic cavity compared to that of the dog, and even more than that of ungulate domestic species where the angle is 30°. Felines are known to have “lazy hearts” where the heart is situated almost horizontally (Tilley, 2008). It has been reported that there is a correlation between heart function and shape (Rowlatt, 1990). Animals with a more pointed heart are more likely to be able to run for prolonged periods compared to animals with a less pointed heart (Lechner, 1942). The domestic cat heart is roughly pear-shaped with the *Apex cordis* lying slightly to the left in the thorax (Hudson & Hamilton, 1993). However, the significance of the oblique angle of the lion heart as well as the blunt shape and positioning of the apex could not be determined in the present study.

The four heart valves used in auscultation for all mammalian species are the left and right atrioventricular valves, and the aortic and pulmonary trunk valves (Miller et al., 1964). The location where the valves can be auscultated the clearest, the *Puncta maxima* (Dyce et al., 2010), is based on the anatomical location of the heart valves. Auscultation of each valve in the domestic cat is difficult as the heart is only about 4 cm in length (Habel, 1978). The *Puncta maxima* in the African lion of the pulmonary valve can be auscultated on the left side of the animal just caudal to the tricipital line. This corresponds with the 4th intercostal space, halfway between the dorsal vertebral attachment of the ribs and the angle in the costal cartilage of rib 4 and 5 (present study). This is slightly more caudal compared to the generalised location for most domesticated species (cat, dog, horse, pig and ruminant) which is in the lower part of the third intercostal space on the left (Habel, 1978). The aortic valve can be auscultated on the left at a slightly higher level in the 5th intercostal space. Again it is noted that the location of this valve is more caudal than the summarised location for domestic species which is high in the fourth intercostal space at the level of the shoulder joint (Habel, 1978). The mitral or left atrioventricular valve in the lion is also located on the left at the 6th intercostal space at the level of the costochondral junction of rib 6. In the dog it is low in the 5th intercostal space at the costochondral junction of rib 5 (Habel, 1978). When compared to the above data it is clear that most of the significant thoracic landmarks for auscultation the lion are located more caudally compared to that of most other domestic species.

The heart of the lion was not as rotated around the vertical axis as noted in other domestic species; the *Atrium dextrum* and *Ventriculus dexter* were on the right side and the *Atrium sinistrum* and *Ventriculus sinister* on the left. This may be related to ventricular size, as it has been reported that a broader *Ventriculus dexter* was present in bears and dogs compared to that of felines. However, it has been noted that this phenomenon does not necessarily represent a functional adaptation but may rather be due to the timing of development during ontogeny (Rowlatt, 1968). Additionally, the right side of the heart is relatively free of major coronary vessels, and together with the larger cardiac incisure makes this a safer entry point for pericardiocentesis or intracardiac injection in the African lion.

4.2 | Pericardium

While the pericardium is not essential for life it plays a role in stabilization of the heart in a fixed position (Spodick, 1983; Hudson & Hamilton, 1993). The pericardium is also a significant structure in various pathologies and peritoneopericardial diaphragmatic hernia (PPDH) is classified as the most common congenital anomaly of the diaphragm and pericardium in dogs and cats (Reimer et al., 2004). Despite dogs and cats demonstrating a *Lig. phrenicopericardiacum,* there is a significant distance between the pericardium and diaphragm, thus the cause of PPDH is unlikely to be induced by trauma but is rather congenital in nature due to the defective development of the *Septum transversum* (Hicks & Britton, 2013). The pericardium of the lion heart has both a sternal and diaphragmatic attachment. The attachment to the diaphragm is broad, yet not directly fixed, as reported in the human (Hicks & Britton, 2013) and thus traumatic PPDH in the lion may also be unlikely. Another mammal reported to possess both the sternal and diaphragmatic pericardial attachment is the ringed seal (*Phoca hispida*), which has a heart that is slightly adapted for diving, with a thin right ventricular wall to assist in coping with the increased pulmonary resistance during diving (Smodlaka et al., 2008). The pericardial ligaments in the lion are delicate, yet have a broad attachments (see Figure 1), and together with the lung tissue surrounding it, may stabilize the heart in the more voluminous caudal thoracic cavity.

4.3 | External features

The exterior of the lion heart is similar to that of the domestic dog and cat. The three grooves on the exterior of the heart that separates the atria and ventricles to form the four heart chambers are similar (Hudson & Hamilton, 1993). A noticeable difference, however, is in the blood supply to the heart wall. Although the circulation of the heart can demonstrate great variability (Bertho & Gagnon, 1964; Lelovas et al., 2014), it is of little importance in veterinary medicine (König & Liebich, 2020). However, of academic interest, the lion has a dominant right coronary artery, while in the dog (Miller et al., 1964) and domestic cat (Hudson & Hamilton, 1993) the left coronary artery supplies a larger portion of the heart.

Similar to the domestic cat, dog and the pig (König & Liebich, 2020), the lion displays an independent left subclavian artery arising from the *Arcus aortae* just distal to the *Tr. brachiocephalicus*. In the foetal circulation, the *Ductus arteriosus* connects the *Tr. pulmonalis* and the *Arcus aortae*. After birth this structure closes and becomes the *Lig. arteriosum* to allow a complete double circulation (Crouch, 1969). Patent *Ductus arteriosus* (PDA) is an anatomical anomaly which is more common in dogs than cats and is characterised by a communication between the *Arcus aortae* and the *Tr. pulmonalis* after birth (Saunders & Birch, 2015). It was noted that between individual cats the anatomical location of PDA differed and that surgical ligation was the best treatment option (Saunders & Birch, 2015). Although the sample size in the present study was small, the position of the *Lig. arteriosum* was consistent in all of the specimens and the surgical approach from the left side for a PDA would be recommended in the lion. The exact surgical incision point may vary between cases as it is common for the arterial ligament location to vary in domestic cats, however, based on this study (in 3 year-old lions) the incision point should be in the 5th intercostal space between rib 5 and 6 slightly dorsal to the costochondral junction of rib 5. This information can assist in future cases of PDA as it has been reported previously in a lion cub which simultaneously displayed a patent *For. ovale* (Franklin, 1946).

4.4 | Internal features

Impulses from the vagus nerve have been reported to work directly on the sinuatrial node and the first point of excitation in the heart is in the auricle (Lewis et al., 1914; Ho & Sanchez-Quintana, 2009). No distinction can be made as to which auricle contracts first because in both auricles there are certain points that contract before its counterpart (Lewis et al., 1914). The distribution of the *Mm. pectinati* in both auricles suggest that the larger contraction would be generated in the right auricle and atrium as the *Mm. pectinati* are more prominent. This larger contraction may be devoted to creating a negative pressure to draw blood inwards from the cranial and caudal vena cava as the atrium is a reservoir for blood to the ventricles (Rowlatt, 1968). Thus the prominent *Mm. pectinati* in the right auricle and atrium noted in the lion heart (present study), may afford a greater ability to rapidly increase cardiac output.

Regarding the thickness of the ventricular walls, the lion heart follows the normal standard of the left ventricular wall being thicker than the right. This is mainly due to the *Ventriculus dexter* performing the function of a “volume pump” and the *Ventriculus sinister* acting as a “pressure pump”, thus requiring a thicker wall to contract and create the required pressure (Rowlatt, 1968).

The *M. papillaris magnus* has an increased muscle length and size, in comparison to the *Mm. papillares parvi*, allowing for a greater force of contraction (Sonnenblick, 1962). This was also noted in the present study in that the larger *M. papillaris magnus* in the right ventricle wall will experience more strain in comparison to the smaller *M. papillaris parvi* attached to the septum, as the *M. papillaris magnus* is required to contract and move as the heart wall moves.

In conclusion the morphology of the lion heart follows the general mammalian standard. However, there are a few topographical and structural adaptations which support the described behaviour of the African lion. The heart is located more caudally in the thorax. This is most likely as a result of the markedly narrowed cranial thoracic cavity, which allows more attachment space for the powerfully

muscled thoracic limbs used in bringing down prey. The well-muscled auricles would most likely aid in increasing cardiac output to support bursts of extreme activity during hunting. Lastly, the heart is stabilised within the thorax by a broad membranous attachment to both the sternum and the diaphragm.

ACKNOWLEDGEMENTS

The authors thank the University of Pretoria for funding the study.

ORCID

Martina Rachel Crole
https://orcid.org/0000-0001-7281-3615

REFERENCES

AZA Lion Species Survival Plan (2012). Lion Care Manual. Association of Zoos and Aquariums: Silver Spring, MD.

Barnett, R., Yamaguchi, N., Barnes, I. & Cooper, A. (2006). Lost populations and preserving genetic diversity in the lion *Panthera leo*: Implications for its ex situ conservation. Conservation Genetics, 7, 507-514.

Bauer, H., Packer, C., Funston, P. F., Henschel, P. & Nowel, K. (2016). *Panthera leo* (errata version published in 2017) [Online]. The IUCN Red list of threatened species 2016: e.T15951A115130419. Available: http://dx.doi.org/10.2305/IUCN.UK.2016-3.RLTS.T15951A107265605.en [Accessed 17 May 2018].

Bauer, H. & Van der Merwe, S. (2004). Inventory of free-ranging lions *Panthera leo* in Africa. Oryx, 38, 26-31.

Bertho, E., & Gagnon, G. (1964). A comparative study in three dimension of the blood supply of the normal interventricular septum in human, canine, bovine, porcine, ovine and equine heart. Diseases of the Chest, 46, 251–262. doi:10.1378/chest.46.3.251

Boyd, J. S., Paterson, C. & May, A. H. (1991). A color atlas of clinical anatomy of the dog & cat. London: Wolfe Publishing Ltd.

Crouch, J. E. (1969). Text-atlas of cat anatomy. Philadelphia: Lea and Febiger.

Chaos the Lion, 2019. https://youtu.be/407tCcL2fZY. Accessed 11 June 2019.

Davis, B. W., Li, G. & Murphy, W. J. (2010). Supermatrix and species tree methods resolve phylogenetic relationships within the big cats, Panthera (Carnivora: Felidae). Molecular Phylogenetics and Evolution, 56, 64-76.

Dyce, K. M., Sack, W. O., & Wensing, C. J. G. (2010). Textbook of veterinary anatomy (4th ed.). Missouri: Saunders Elsevier.

Franklin, K. (1946). Patent foramen ovale and ductus arteriosus in a lion cub. Journal of Anatomy, 80, 209.

Goldin, J. P., & Lambrechts, N. E. (1999). Double aortic arch and persistent left vena cava in a white lion cub (*Panthera leo*). Journal of Zoo and Wildlife Medicine, 30, 145-150.

Habel, R. E. (1978). Applied veterinary anatomy (2nd ed.). Michigan: Edwards Brothers Inc.

Hartman, M. J., Groenewald, H. B., & Kirberger, R. M. (2013). Morphology of the female reproductive organs of the African lion (*Panthera leo*). Acta Zoologica, 94, 437-446.

Hartstone-Rose, A., Long, R. C., Farrell, A. B. & Shaw, C. A. (2012). The clavicles of *Smilodon fatalis* and *Panthera atrox* (Mammalia: Felidae) from Rancho La Brea, Los Angeles, California. Journal of Morphology, 273, 981-991.

Heath, D. (2019). Hunting lion. Retrieved from https://www.norma.cc/en/About-Norma/About-Hunting/Plains-game-hunting/hunting-lion/

Hicks, K. A., & Britton, A. P. (2013). A fatal case of complicated congenital peritoneopericardial diaphragmatic hernia in a Holstein calf. The Canadian Veterinary Journal, 54, 687-689.

Ho, S., & Sanchez-Quintana, D. (2009). The importance of atrial structure and fibers. Clinical Anatomy, 22, 52-63.

Hopwood, A. T. (1947). Contributions to the study of some African Mammals.—III. Adaptations in the bones of the fore-limb of the Lion, Leopard, and Cheetah. Zoological Journal of the Linnean Society, 41, 259-271.

Hudson, L. C., & Hamilton, W. P. (1993). Atlas of feline anatomy for veterinarians. Philadelphia: W.B. Saunders Company.

ICVGAN (International Committee on Veterinary Gross Anatomical Nomenclature) (2012). World association of veterinary anatomists: Nomina anatomica veterinaria. (5th ed.) Hannover, Germany: The Editorial Committee.

Kirberger, R. M., Du Plessis, W. M. & Turner, P. H. (2005a). Radiologic anatomy of the normal appendicular skeleton of the lion (*Panthera leo*). Part 1: Thoracic limb. Journal of Zoo and Wildlife Medicine, 36, 21-28.

Kirberger, R. M., Du Plessis, W. M. & Turner, P. H. (2005b). Radiologic anatomy of the normal appendicular skeleton of the lion (*Panthera leo*). Part 2: Pelvic limb. Journal of Zoo and Wildlife Medicine, 36, 29-35.

König, H.E. & Liebich, H.-G. (2020). Veterinary anatomy of domestic animals. Textbook and colour atlas (7th ed.). Stuttgart: Thieme Publishing Group.

Lechner, W. (1942). Herzspitze und Herzwirbel. Anatomische Anzeiger, 92, 249-283.

Lelovas, P. P., Kostomitsopoulos, N. G., & Xanthos, T. T. (2014). A comparative anatomic and physiologic overview of the porcine heart. Journal of the American Association for Laboratory Animal Science, 53, 432-438.

Lewis, T., Meakins, J., & White, P. D. (1914). X. The excitatory process in the dog's heart. Part I.—The auricles. Philosophical Transactions of the Royal Society of London. B, 205, 375-420.

Lindsey, P. A., Alexander, R., Frank, L., Mathieson, A. & Romañach, S. (2006). Potential of trophy hunting to create incentives for wildlife conservation in Africa where alternative wildlife-based land uses may not be viable. Animal Conservation, 9, 283-291.

Lindsey, P. A., Alexander, R., Mills, M. G. L., Romañach, S. & Woodroffe, R. (2007a). Wildlife viewing preferences of visitors to 12 protected areas in South Africa: Implications for the role of ecotourism in conservation. Journal of Ecotourism, 6, 19-33.

Lindsey, P. A., Roulet, P. & Romañach, S. (2007b). Economic and conservation significance of the trophy hunting industry in sub-Saharan Africa. Biological Conservation, 134, 455-469.

Loveridge, A., Searle, A., Murindagomo, F. & MacDonald, D. (2007). The impact of sport-hunting on the population dynamics of an African lion population in a protected area. Biological Conservation, 134, 548-558.

Luckhaus, G. (1969). Vergleichend-anatomische Betrachtungen über den Pharynx des Löwen: mit Berücksichtigung der mikroskopischen Anatomie seiner Tonsilla palatina. Transboundary and Emerging Diseases, 16, 240-256. https://doi.org/10.1111/j.1439-0442.1969.tb00726.x

Macdonald, A., & Johnstone, M. (1995). Comparative anatomy of the cardiac foramen ovale in cats (Felidae), dogs (Canidae), bears (Ursidae) and hyaenas (Hyaenidae). Journal of Anatomy, 186, 235-243.

Miller, M. E., Christensen, G. C., & Evans, H. E. (1964). Anatomy of the dog. Philadelphia: W. B. Saunders Company.

Novales, M., Ginel, P., Diz, A., Blanco, B., Zafra, R., Guerra, R. & Mozos, E. (2015). Mucoperiosteal exostoses in the tympanic bulla of African lions (*Panthera leo*). Veterinary Pathology, 52, 377-383.Peters, G. & Hast, M. (1994). Hyoid structure, laryngeal anatomy, and vocalization in felids (Mammalia: Carnivora: Felidae). Zeitschrift für Saugetierkunde, 59, 87-104.

Reimer, S. B., Kyles, A. E., Filipowicz, D. E., & Gregory, C. R. (2004). Long-term outcome of cats treated conservatively or surgically for peritoneopericardial diaphragmatic hernia: 66 cases (1987–2002). Journal of the American Veterinary Medical Association, 224, 728-732.

Rowlatt, U. (1990). Comparative anatomy of the heart of mammals. Zoological Journal of the Linnean Society, 98, 73-110.

Rowlatt, U. (1968). Functional morphology of the heart in mammals. American Zoologist, 8, 221-229.

Saunders, A. B., & Birch, S. A. (2015). Three-dimensional modeling of a patent ductus arteriosus in a cat. Journal of Veterinary Cardiology, 17, S349-S353. doi:https://doi.org/10.1016/j.jvc.2015.08.006

Schaller, O. (1991). Illustrated veterinary anatomical nomenclature (2nd ed.) Stuttgart, Germany: Thieme Publishing Group.

Smodlaka, H., Henry, R., Schumacher, J., & Reed, R. (2008). Macroscopic anatomy of the heart of the ringed seal (*Phoca hispida*). Anatomia Histologia Embryologia, 37, 30-35.

Sonnenblick, E. H. (1962). Force-velocity relations in mammalian heart muscle. American Journal of Physiology-Legacy Content, 202, 931-939.

Spodick, D. H. (1983). The normal and diseased pericardium: current concepts of pericardial physiology, diagnosis and treatment. Journal of the American College of Cardiology, 1, 240-251.

Steeil, J.C., Schumacher, J., Baine, K., Ramsay, E.C., Sura, P., Hodshon, R., Donnell, R.L., & Lee, N.D. (2013). Diagnosis and treatment of a dermal malignant melanoma in an African lion (*Panthera leo*). Journal of Zoo and Wildlife Medicine, 44, 721-727.

Thrall, D. E., & Robertson, I. D. (2011). Atlas of normal radiographic anatomy and anatomic variants in the dog and cat (S. Stringer Ed. 1st ed.). Missouri: Elsevier Saunders.

Tilley, L. P. (2008). Manual of canine and feline cardiology. St. Louis, Missouri: Elsevier Health Sciences.

Weissengruber, G. E., Forstenpointner, G., Peters, G., Kübber-Heiss, A. & Fitch, W. T. (2002). Hyoid apparatus and pharynx in the lion (*Panthera leo*), jaguar (*Panthera onca*), tiger (*Panthera tigris*), cheetah (*Acinonyx jubatus*) and domestic cat (*Felis silvestris f. catus*). Journal of Anatomy, 201, 195-209.

Where to find this article: Marais CA, Crole MR. Gross morphology of the African lion (*Panthera leo*) heart. *Acta Zool*. 2021;00:1–12. https://doi.org/10.1111/azo.12381